

## RESEARCH ARTICLE



# A Multipath Approach to Self-Interference Cancellation in MIMO Rayleigh Fading Channels

Archa Chandrasenan<sup>1,\*</sup> and Joseph Zacharias<sup>1</sup>

<sup>1</sup>College of Engineering Trivandrum, APJ Abdul Kalam Technological University (Kerala), India

**Abstract:** An optically enabled multipath self-interference (MSI) cancellation technique for in-band full duplex (IBFD) multiple input multiple output (MIMO) Radio over Fiber RoF systems under Rayleigh fading channels is proposed. A digitally assisted Rayleigh fading channel model generates the MSI signal. An optically tunable multipath delay lines (OTMDL) module is designed using optical delay lines and an optical attenuator for coarse and fine-tuning of time delays and amplitude matching between the locally generated reference (LR) signal and the MSI signal. The OTMDL module adjusts the LR signal to cancel the effect of MSI on the signal received through the fading channel. The concept is validated using a remote sensor node of a  $3 \times 3$  IBFD MIMO RoF system with a Rayleigh fading channel. The system's performance is evaluated by determining the MSI cancellation depths using the OTMDL section for various cancellation channels and by computing the MSI cancellation for both single band and wideband signals across different cancellation channels. An average value of MSI cancellation depth of 20.38 dB is obtained for a single-tone radio frequency signal in the range 15–25 GHz. Thus, the proposed system for MSI cancellation can be utilized in wireless communication systems in multiple ways.

**Keywords:** in-band full duplex, multipath, self-interference, optical delay line, optical attenuator

## 1. Introduction

The rapid growth in the number of smartphone users, average data traffic per smartphone, and rise in data-intensive content may lead to a five-fold increase in global mobile data traffic between 2022 and 2027. This creates significant spectrum incompatibility issues and increases the pressure on the current mobile infrastructure to keep up with the growing demand for mobile services. These incompatibility issues necessitate new and innovative solutions to find more spectrum resources, such as developing traditional spectrum-sharing techniques and exploring new ones.

Recently, in-band full-duplex (IBFD) multiple input multiple output (MIMO) technology has emerged as a promising solution for the spectrum congestion problem. IBFD MIMO technology allows the system to transmit and receive simultaneously in the same frequency band, using different antennas for transmission and reception. This facilitates straightforward management of the spectrum and has various applications, including vehicular communication, heavy equipment operation, cognitive radio, and heterogeneous networking. However, IBFD MIMO communication systems have not seen widespread use due to their potential debilitating effects of co-site multipath self-interference (MSI). MSI is generated by all transmitting signals

from each transmitter section into each receiver section. Most of the time, the power of MSI is significantly greater than the signal of interest (SOI) received by the receiver. Thus, MSI affects link scheduling, reduces overall network capacity, minimizes dynamic range, and degrades receiver sensitivity. To overcome the problem of MSI in IBFD MIMO systems, several cancellation techniques have been proposed in propagation domain [1], analog domain [2], and digital domain [3]. Propagation domain MSI cancellation techniques include impedance tuning of antennas [4], cross-polarization techniques [5], and transmitter beamforming methods [6]. Analog domain MSI cancellation systems employ balanced/unbalanced transformers [7], opamps [8], programmable passive attenuators [9], passive delay lines, amplifiers, and passive inverters. However, analog domain MSI cancellation techniques alone are unable to meet the demand for large bandwidth and high frequency in future 5G wireless communication systems. The cost, size, and complexity of an MSI cancellation system are predominantly based on components used in the analog field [10].

Digital domain-based MSI cancellation technique is applied for processing weak signals with delays greater than 1000 ns to cancel residual interference and obtain an error-free representation of the channel. In the literature of Urick et al. [11], a photonics-based approach for simultaneous adaptive radio frequency (RF) self-interference cancellation (SIC) and frequency down conversion is described. The technique utilizes photonic polarization-multiplexing to separate the reference signal and self-interference signal in the optical domain. This allows for precise adjustments

\*Corresponding author: Archa Chandrasenan, College of Engineering Trivandrum, APJ Abdul Kalam Technological University (Kerala), India. Email: archachandrasenan@cet.ac.in

in phase shift, amplitude, and time delay using optical methods that can be programmed and controlled. In the study of Han et al. [12], the particle swarm optimization algorithm is applied to achieve adaptive RF-SIC and frequency down conversion in a photonic system. The technique introduces a local oscillator signal to two orthogonal polarization states, allowing for simultaneous cancellation of self-interference and down conversion of the desired RF signal. This approach offers advantages in terms of programmability, control, and simultaneous operation. The characteristic of bidirectional signal transparency of  $N$ -phase passive mixer and a mixer-first active electrical balance self-interference suppression architecture is proposed. The solution is cost-effective and space-saving as it does not require a costly and space-consuming out-of-chip circulator. To alleviate the multipath effect, a two-tap baseband self-interference suppression is adopted, which also helps broaden the self-interference suppression bandwidth [13]. Moreover, the SI channel exhibits a large multipath delay spread in these applications, especially in UHF-band terrestrial broadcasting systems where the transmission frequency is lower and the antenna directivity is limited [14].

A novel iterative successive nonlinear SI cancellation scheme based on the previously proposed frequency-domain RF-SIC technique is presented in the literature of Hong et al. [15]. Additionally, a photonics-assisted adaptive MSI cancellation scheme using deep reinforcement learning (DRL) is proposed and experimentally demonstrated [16]. Multiple local reference signals are obtained using optical wavelength division multiplexing to achieve MSI cancellation. An adaptive algorithm based on DRL is applied for adaptive optimization of multi-dimensional optical parameters to achieve real-time MSI cancellation [17]. In this paper, we propose and demonstrate a photonics-based MSI cancellation technique for the RoF system based on IBFD MIMO architecture under the Rayleigh fading channel. The reference signals are generated locally at the remote sensors and modulated using a Mach-Zehnder modulator (MZM) at various optical frequencies. These modulated signals are fed into a wavelength division multiplexer (WDM), where they are multiplexed into extremely tight wavelength spacing. The multiplexed signals are then given to optically tunable multipath delay lines (OTMDL), where the amplitude and time delay of each signal are specifically adjusted. The channels from the OTMDL module are multiplexed using another WDM, forming the MSI cancellation signal. This combined signal is used to cancel all MSI signals. The Rayleigh fading model is used to represent the multipath channel, where the received signal is composed of multiple random components due to reflections and scattering by various obstacles. Our proposed method aims to cancel the effect of MSI by optically calibrating time delays and amplitude attenuation. This scheme balances receiver complexity and system performance, and our results have shown that it can outperform conventional IBFD systems. The results obtained substantiate the feasibility of our proposed work. Under the Rayleigh multipath fading channel of IBFD  $3 \times 3$  MIMO RoF signal transmission, we achieved MSI cancellation depths of 41.25, 38.45, 35.23, and 28.91 dB at 20 GHz for bandwidths of 100 MHz, 500 MHz, 1 GHz, and 2 GHz respectively. This paper is structured as follows: Section 2 discusses the principle of our proposed system. Section 3 provides details about the implementation of our system. Section 4 gives an analysis of the results obtained. Finally, Section 5 concludes the paper.

## 2. Principle

Our proposed method for MSI cancellation in a standard IBFD MIMO RoF transmission system based on photonics is schematically illustrated in Figure 1. A typical IBFD MIMO RoF transmission system has central units (CUs), optical fiber-based transmission links, and remote sensing units (RSUs). The CU has transmitting RoF section (TRS) and MSI cancellation section (MSICS). The RSU has transmitting antenna section (TAS) and receiving antenna section (RAS). The RAS receives the SOI, which is affected by a strong MSI signal. To remove the MSI effect, we use MSICSs in the CU. The downlink transmission (DL) is from TRS to TAS. In TRS, we use a continuous wave laser diode (CW-LD) as the optical source. We adjust the polarization and feed the optical carrier signal from CW-LD into an MZM to modulate the information signal. We operate the MZM at the quadrature bias point to improve the spurious-free dynamic range. We multiplex the modulated signal from each TRS using WDM for easy reconfiguration and higher bandwidth utilization. We use an optical coupler (OC) to split the multiplexed signal from TRSs into two optical paths. One path is the DL signal to TAS and the other is the locally generated reference (LR) signal.

The mathematical expression of the multiplexed optical signal from TRSs is given by Equation (1) [4]

$$E_1(t) \propto E_c \sum_{i=1}^n \exp^{j(2\pi f_i t)} \left[ \exp^{jm_i(\cos(2\pi f_{RF}t + \theta))} + \exp^{-jm_i(\cos(2\pi f_{RF}t))} \right] \quad (1)$$

where  $E_1(t)$  is the optical transmitting signals,  $E_c$  is the amplitude of the optical carrier signal from CW-LD at the TRS,  $m_i = \pi V_i(t) / V_\pi$ ,  $V_i(t)$  is the amplitude of the wideband signal,  $V_\pi$  is the half-wave voltage of MZM,  $f_i$  is the frequency of the optical carriers,  $f_{RF}$  is the frequency of the wideband signal, and  $i$  is the range of channels.

The multiplexed signal is fed to SM-OF and MSICS using OC for downlink transmission and cancellation of MSI, respectively. At TASS, the incoming signal is demultiplexed and converted to electrical signals before being fed to transmitting antennas [10].

Using Jacobi-Anger expansion and assuming the condition of small signal approximation, Equation (1) can be rewritten as

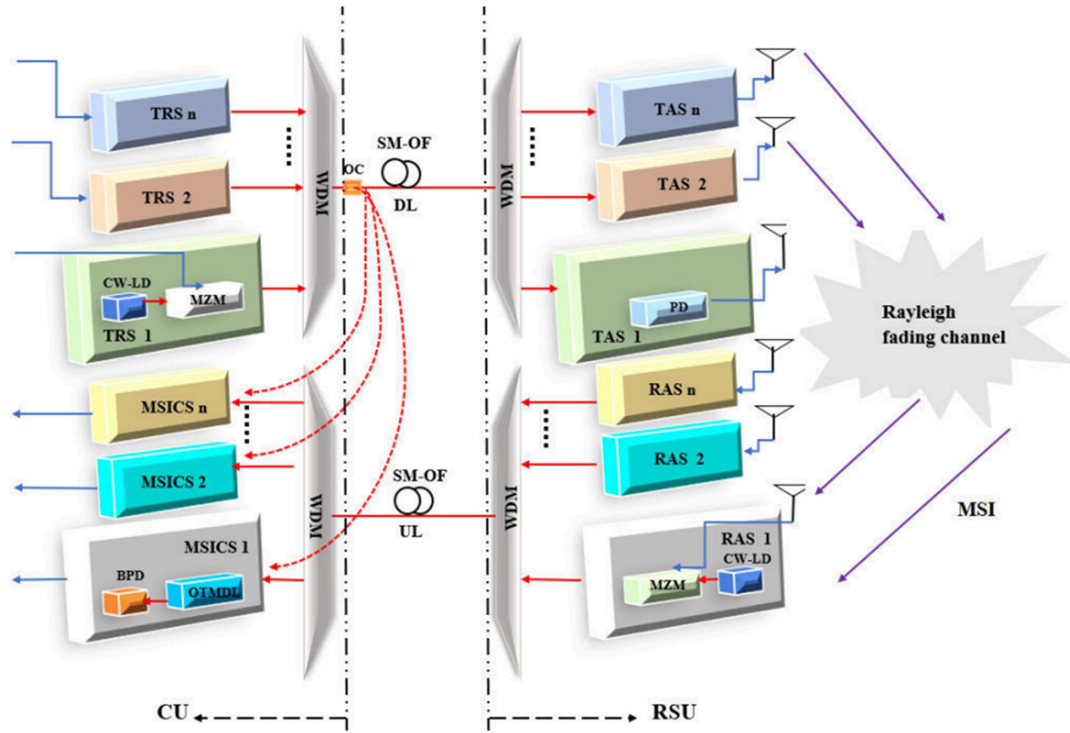
$$E_1(t) \propto E_c \sum_{i=1}^n \exp^{j(2\pi f_i t)} [J_0(m_i) - J_1(m_i)\exp^{j(2\pi f_{RF}t)} - J_1(m_i)\exp^{-j(2\pi f_{RF}t)}] \quad (2)$$

where  $J_n$  is the  $n$ th-order Bessel function of the first kind. The transmitted signal from TAS is passed through the fading channel and is received by the receiver antennas, which is located at RAS.

A Rayleigh fading-based wireless channel is used to simulate the real-world scenario of multipath signal transmission. The signal transmitted from the TASS passes through this channel to reach the RAS. The signal is affected by multipath scattering effects, time dispersion, and Doppler shifts as it travels through the wireless channel [10]. A baseband channel model for a multipath propagation scenario is created using  $n$  discrete fading paths with the Rayleigh model. Each path has a specific time delay and an average power gain. The wireless multipath channel is modeled using a Jakes Doppler spectrum. The multipath fading channel is implemented assuming that the delay power profile and

Figure 1

Diagrammatic representation of the proposed photonic assisted multipath self-interference cancellation technique for MIMO-based RoF communication system working on IBFD mode



**Note:** TRS: transmitter RoF section, TAS: transmitting antenna section, RAS: receiving antenna section, MSICS: multipath self-interference cancellation section, LD: laser diode, MZM: Mach–Zehnder modulator, PD: photodetector, OTMDL: optically tunable multipath delay lines, SM-OF: single mode optical fiber, UL: uplink transmission, DL: downlink transmission, CU: central unit, RSU: remote sensory unit

the Doppler spectrum of the channels are separable. It is modeled as a linear finite impulse response filter with  $s_i$  and  $s_o$  as the set of samples at the input and output of the channel, respectively. They are related by  $s_o = \sum_{n=-N_1}^{N_2} s_i - n g_n$ , where  $g_n$  is the set of tap weights given by  $g_n = \sum_{k=1}^n a_k \text{sinc} \left[ \frac{\tau_k}{T_s} - n \right]$ ,  $-N_1 \leq n \leq N_2$ .  $T_s$  is the input sample period to the channel,  $\tau_k$  is the set of path delays,  $a_k$  is the set of complex path gains of the multi path fading channel,  $N_1$  and  $N_2$  are chosen so that  $g_n$  is small, and  $n$  is the total number of paths in the multi path fading channel [7].

The uplink transmission (UL) is initiated from RASs to MSICSs. CW-LD along with MZM is used at the RAS to modulate the electrical signal received by the receiver antennas. The received signal from antennas consists of the downlink information signal affected by MSI. The modulated signal from RASs is multiplexed using WDM and transmitted to the MSICS sections, which are located at the CU side. The modulated optical signal from the output of RASs is given by Equation (3)

$$E_2(t) \propto E_c \sum_{i=1}^n \exp^{j(2\pi f_i t)} \left[ \exp^{j\mu_i (\cos(2\pi f_{RF}(t+\tau_{u,i})+\theta))} + \exp^{-j\mu_i (\cos(2\pi f_{RF}(t+\tau_{u,i}))} \right] \quad (3)$$

where  $\mu_i = \frac{\pi \alpha_{u,i} V_i (t+\tau_{u,i})}{V_\pi}$ ,  $u$  represents the uplink transmission,  $\tau_{u,i}$  is the time delay, and  $\alpha_{u,i}$  is the signal attenuation of the uplink multi-

path signals. Under small signal approximation, the signal from RASs is rewritten as

$$E_2(t) \propto E_c \sum_{i=1}^n \exp^{j(2\pi f_i t)} \left[ J_0(\mu_i) \exp^{j\theta_{0,0}} - J_1(\mu_i) \exp^{j(2\pi f_{RF}(t+\tau_{u,i})+\theta_{+1,0})} - J_1(\mu_i) \exp^{-j(2\pi f_{RF}(t+\tau_{u,i})+\theta_{-1,0})} \right] \quad (4)$$

where  $\theta_{n,0} = \beta L + n\tau\omega_{RF} + \frac{n}{2} |D\omega_{RF}^2|$  are the phases of the optical carriers affected by dispersion.  $\beta$  is the zero-order derivative of the propagation constant with respect to optical angular frequency  $\omega_{RF}$ ,  $L$  is the distance traveled by the signal,  $\tau$  is the signal group delay, and  $n$  is the order side bands of the self-interference signals caused by Rayleigh multipath fading channel [18].

Signals from various RASs are multiplexed, transmitted through an optical fiber, and fed into the MSICS section. The MSICS section contains a proposed MSI cancellation system that uses an OTMDL module to effectively cancel the effect of MSI on the received signal. The OTMDL module densely demultiplexes the signal (as given by Equation (2)) and serves as the local reference signal. An optically variable time delay line (OVDL) module finely inserts a time delay ( $\tau_{r,i}$ ) into the signal using multiple sections of optical fiber lines (OFLs).

An optically variable amplitude attenuator (OVA) is used to insert attenuation ( $\alpha_{r,i}$ ) into the amplitude of the local reference signal.

The matched signal from the output of OTMDL module is given by Equation (5)

$$E_3(t) \propto E_c \sum_{i=1}^n \alpha_{r,i} \exp^{j(2\pi f_i(t+\tau_{r,i}))} \left[ J_0(\delta_i) - J_1(\delta_i) \exp^{j(2\pi f_{RF}(t+\tau_{r,i}))} - J_1(\delta_i) \exp^{-j(2\pi f_{RF}(t+\tau_{r,i}))} \right] \quad (5)$$

where  $\delta_i = \frac{\pi V_i(t+\tau_{r,i})}{V_\pi}$ . To cancel the MSI signal, the received signal from RAS containing the MSI (Equation (4)) and the local reference signal from OTMDL (Equation (5)) are fed to BPD [19]. The photo-detected signal is given as

$$I \propto \sum_{i=1}^n A_i \cos(2\pi f_{RF} T_1) - \sum_{i=1}^n B_i \cos(2\pi f_{RF} T_2) \quad (6)$$

where  $A_i = \frac{\alpha_{u,i} V_i(T_1)}{V_\pi} \cos(D4\pi^2 f_{RF}^2 T_1)$  and  $B_i = \frac{\alpha_{u,i} V_i(T_2)}{V_\pi}$ . From Equation (6), we can see that the effect of MSI signal can be canceled by precisely tuning the OVDL module to make  $T_1 = T_2$ , where  $T_1 = t + \tau_{u,i} + \tau$  and  $T_2 = t + \tau_{r,i}$ , and adjusting the OVA module such that  $\alpha_{u,i} \cos(D4\pi^2 f_{RF}^2 T_1) = \alpha_{r,i}^2$  [20].

The proposed system presents several advantages over existing self-cancellation methods. It effectively eliminates inter-carrier interference and boasts high bandwidth efficiency, making it the perfect solution for maximizing data transmission within a limited spectrum. It also exhibits a low bit error rate over multipath fading channels, ensuring dependable communication even in challenging conditions. Furthermore, it is particularly adept at managing closely spaced multipaths, making it ideal for indoor environment where multipath propagation is prevalent. In summary, the suggested scheme offers a promising solution that enhances signal quality, minimizes errors, and makes efficient use of available bandwidth.

However, there are several factors that may negatively impact the cancellation performance of the proposed system, including signal scattering [20], power fading [21], exposure to radiation [22], and range limitations. To improve performance, pre-compensation and post-compensation techniques, frequency down

conversion mechanisms, and DSP-based algorithmic computations can be implemented [23].

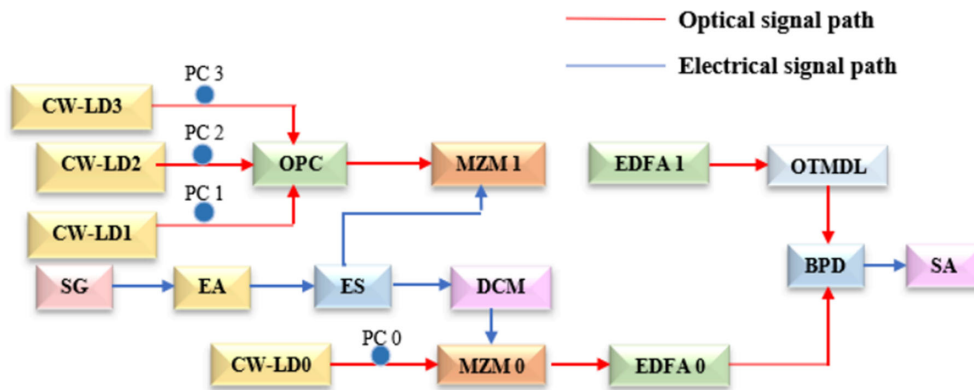
### 3. System Implementation

We conducted a proof-of-concept test based on Figure 2. It shows a single receiver  $3 \times 3$  MIMO RoF system in IBFD mode with a Rayleigh fading channel. We used CW-LD0 to generate an optical carrier of 193.76 THz and 16 dBm power. We modulated it with MZM0 at 4.6 V bias and 5.2 V RF voltage using the signal from digitally assisted channel model (DCM). DCM simulates the wideband multipath Rayleigh fading channel with spectral characteristics. We created the wideband SOI with signal generator (SG) and amplified it with an electrical amplifier of 1.5 dB gain and 45 depths. We split the amplified signal into two branches with an electrical splitter of 3 dB loss and 1:1 power ratio. One branch was the LR signal and the other branch went to DCM. DCM models the Rayleigh fading multipath channel, which is common in wireless communication. It has multipath scattering, time dispersion, and Doppler shifts of diffuse components. DCM has three fading paths, each with a cluster of multipath components. The maximum delay is  $1.5 \times 10^{-5}$  s and the maximum Doppler shift is 200 Hz for diffuse components.

DCM is a baseband channel model for multipath scenarios. It has  $n$  fading paths, each with its own delay and power gain. If  $n$  is more than 1, the channel is frequency-selective for a wideband signal [11]. Each path has a Rayleigh model in this scenario. DCM uses a Jakes Doppler spectrum with zero maximum Doppler shift. The first path has zero delay, while the others have delays between  $1.5 \times 10^{-5}$  s and  $1 \times 10^{-7}$  s. The power gain of each path ranges from  $-20$  to  $0$  dB. The  $K$ -factor is the ratio of specular to scattered power in a fading channel. In DCM, the  $K$ -factor is zero, meaning Rayleigh fading with no specular component and multipath fading.

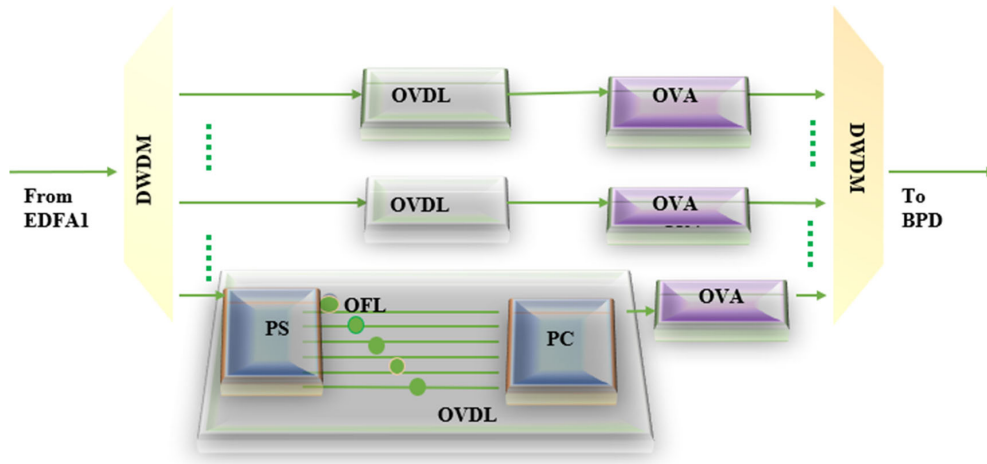
The TRSSs with three sources are modeled using three optical sources, CW-LD1, CW-LD2, and CW-LD3, with frequencies of 193.60, 193.53, and 193.03 THz, respectively, and power levels of 16 dBm. An optical power combiner combines these sources and feeds them to MZM1, which modulates the LR signal with bias voltages of  $-2.8$  and  $-3.5$  V and a modulation voltage of 4.9 V.

**Figure 2**  
Experimental setup of the proposed photonic assisted multipath self-interference cancellation technique



**Note:** CW-LD: continuous wave laser diode, PC: polarization controller, OPC: optical power combiner, MZM: Mach-Zehnder modulator, EDFA: erbium-doped fiber amplifier, OTMDL: optically tunable multipath delay lines, SG: signal generator, EA: electrical amplifier, ES: electrical splitter, DCM: digitally assisted channel model, BPD: balanced photodetector, SA: signal analyzer

Figure 3  
Logic diagram showing the architecture of OTMDL section for multipath cancellation



**Note:** DWDM: dense wavelength division multiplexer, PS: power splitter, PC: power combiner, OVDL: optically variable time delay line, OVA: optically variable amplitude attenuator

MZM0 and MZM1 receive the multipath signal from DCM and the LR signal as their RF input ports, respectively. Two erbium-doped fiber amplifiers (EDFA0 and EDFA1) amplify the modulated signals from MZM0 and MZM1, respectively. EDFA0 and EDFA1 have core radii of 2.5 and 3.6  $\mu\text{m}$ , lengths of 2 and 5 m, and numerical apertures of 0.21 and 0.45, respectively. They help to reduce nonlinearity and crosstalk in data transfer. The OTMDL section's signal port gets the modulated signal from MZM1 after amplification by EDFA1.

The OTMDL section demultiplexes the incoming signal into three closely spaced channels using a  $1 \times 3$  DWDM with a bandwidth of 14 GHz and a depth of 45 dB. Each channel goes through a series of OVAs and optically variable time delay lines (OVDLs). OVA and OVDL can provide low phase noise, a linear adjustment range, a sharp tuning range, and a high precision level. OVDL and OVA have maximum accuracies of 0.52 ps and 0.67 dB, respectively, with tuning ranges from 2 to 10 ns and 5 to 45 dB, respectively. OVDL and OVA modules use microwave photonic integration technology to control the optical path length variation. These modules are easy to assemble and align, requiring only small changes in propagation distance or fiber length on the order of one optical wavelength in each channel for fine-tuning the optical phase [12]. For coarse tuning, a variable time delay controls the relative timing between two ultrashort pulses with a detector signal that measures their function. OVA enables the user to change the signal attenuation for accurate power balancing in fiber circuits or dynamic range evaluation in measurement systems.

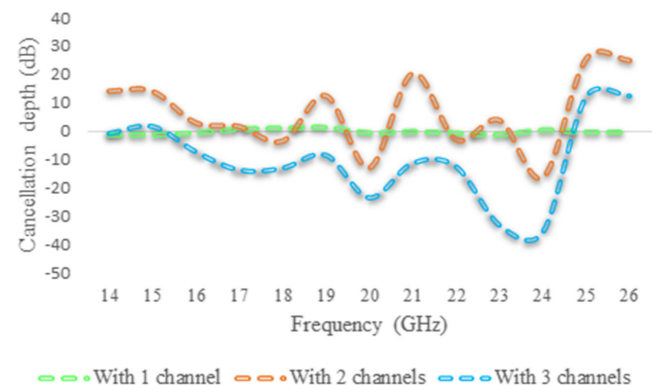
The OTMDL section, which has both OVA and OVDL parts, is shown in Figure 3. The OVDL part has three sets of  $1 \times 6$  PS, six OFLs with different lengths, and a  $6 \times 1$  PC. The PS has a power ratio array of [1 1 1 1 1 1] and an insertion loss of 0.2 dB. The OFLs have lengths from 1/1.5 to 5/5.5 m and the PC has a loss of 0.45 dB. The OVA adjusts the amplitude of the signals, which are then multiplexed by a  $3 \times 1$  DWDM with a bandwidth of 12 GHz and a depth of 25 dB. The OTMDL section's output goes to one input port of the BPD, which has a responsivity of 10 A/W, a gain factor of 3, and an ionization ratio of 0.9. The modulated signal from MZM0 is amplified by EDFA0 and goes to another input port of the BPD. An RF spectrum analyzer monitors the

difference in photocurrents, with a frequency range of 9–7 GHz, a resolution bandwidth of –10 Hz to 3 MHz, and a phase noise of –90 dB/Hz.

#### 4. Result Analysis

We calculated the MSI cancellation depths using the OTMDL section for different numbers of cancellation channels. To verify the MSI cancellation depths of the proposed system, we generated a single-tone RF signal from 15 to 25 GHz with a bias of 5 a.u using SG. We then gave this signal to the proposed system and analyzed the electrical spectra from BPD to validate the MSI cancellation with the number of cancellation channels in the OTMDL module. After calculating the MSI cancellation depths by varying the cancellation channels in the OTMDL module, we plotted Figure 4. This figure shows the cancellation depth of the signal in the generated frequency range using different numbers of channel cancellations. It is noticeable from Figure 4 that as the

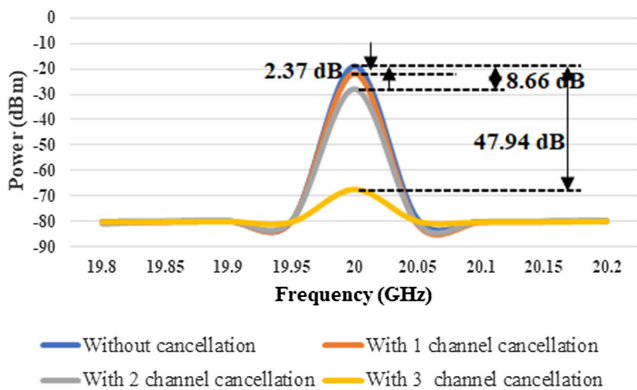
Figure 4  
Calculated multipath self-interference cancellation depths obtained using OTMDL section for different cancellation channels, when the frequency of single-tone RF signal is varied from 15 to 25 GHz



number of cancellation channels varies from 1 to 3, the average value of the cancellation depth ranges from 6.565 to 20.38 dB, respectively. On top of that, we obtained the best possible cancellation depth of 30.63 dB within the frequency range of 16.45 – 19.63 GHz. This shows that our proposed system has stable operation and good MSI cancellation performance for single-tone RF signals in the frequency range of 16.45–19.63 GHz.

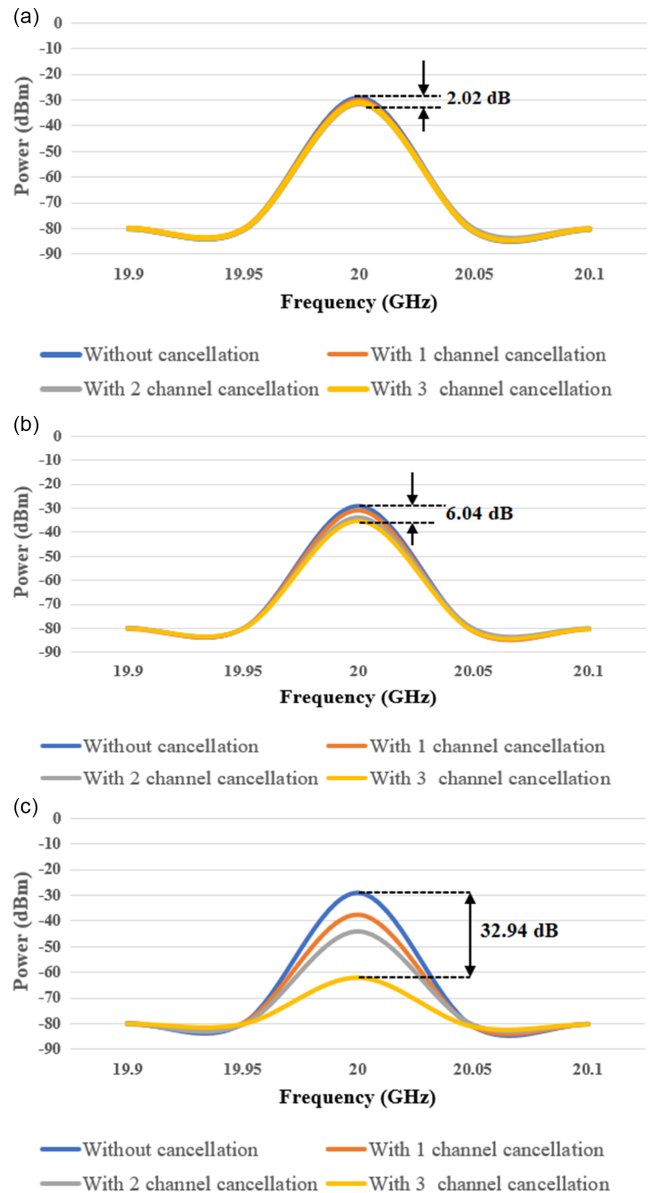
Furthermore, we evaluated the MSI cancellation performance of our proposed system for single-tone frequency signal transmission by generating a 20 GHz signal using SG. Using this generated signal, we calculated the MSI cancellation of our system by operating it with and without an OTMDL module. Moreover, we investigated the effect of MSI cancellation using an OTMDL module by using different cancellation channels in it. The measured spectrum of the photo-detected signal showing MSI cancellation at a carrier frequency of 20 GHz is shown in Figure 5. We can infer that the maximum power of the MSI signal induced by Rayleigh fading channel is  $-18.17$  dBm and it is reduced to  $-21.64$ ,  $-27.93$ , and  $-67.21$  dBm when we set the cancellation channels to 1, 2, and 3, respectively, inside an OTMDL module.

**Figure 5**  
Electrical spectra obtained when single-tone signal at 20 GHz is used for multipath self-interference cancellation at OTMDL section for various cancellation channels



To ascertain our proffered method of MSI cancellation for wideband RF signals, we generated linearly frequency-modulated wideband signals with a center frequency of 20 GHz and bandwidths of 100 MHz, 200 MHz, 500 MHz, and 1 GHz using SG. We then gave a 20 GHz wideband signal with each aforementioned bandwidth to our proposed system to verify its wideband MSI cancellation performance. Figures 6–9 show the electrical spectrum obtained at BPD’s output using different cancellation channels – 0, 1, 2, and 3. From Figure 6, we can gather that for a wideband signal with a center frequency of 20 GHz and bandwidth of 100 MHz, we achieved an MSI cancellation depth of 2.02, 6.04, and 32.94 dB using different numbers of channel cancellations. Similarly, from Figures 7–9, we can conclude that for signals centered at 20 GHz with bandwidths of 200 MHz, 500 MHz, and 1 GHz, respectively, we achieved cancellation depths ranging from 1.91 to 18.55 dB, from 2.61 to 21.46 dB, and from 2.32 to 18.02 dB using different numbers of channel cancellations, respectively. Comparison of MSI cancellation depth obtained for signal with center frequency 20

**Figure 6**  
Electrical spectra obtained of different iterations of wideband multipath self-interference cancellation at carrier frequency of 20 GHz and bandwidth of 100 MHz, under (a) 1 cancellation channel, (b) 2 cancellation channels, and (c) 3 cancellation channels



GHz at different bandwidths vs different number of cancellation channels is given in Table 1.

The depression in the center of the wideband signal after cancellation is caused by the residual self-interference signal that is not completely eliminated. To optimize the overall SIC depth, several measures can be taken, such as using a high-quality RF front-end filter, increasing the number of antennas, and employing advanced SIC algorithms. Certain chirps and residual amplitude fluctuations are seen on the obtained spectrum due to mismatches in time delay and poor matching of high-frequency circuits. Factors such as narrow bandwidth, inadequate flexibility of electronic devices, susceptibility to EMI, and non-uniform correspondence of amplitude and phase lead to degradation of

Figure 7

Electrical spectra obtained of different iterations of wideband multipath self-interference cancellation at carrier frequency of 20 GHz and bandwidth of 200 MHz, under (a) 1 cancellation channel, (b) 2 cancellation channels, and (c) 3 cancellation channels

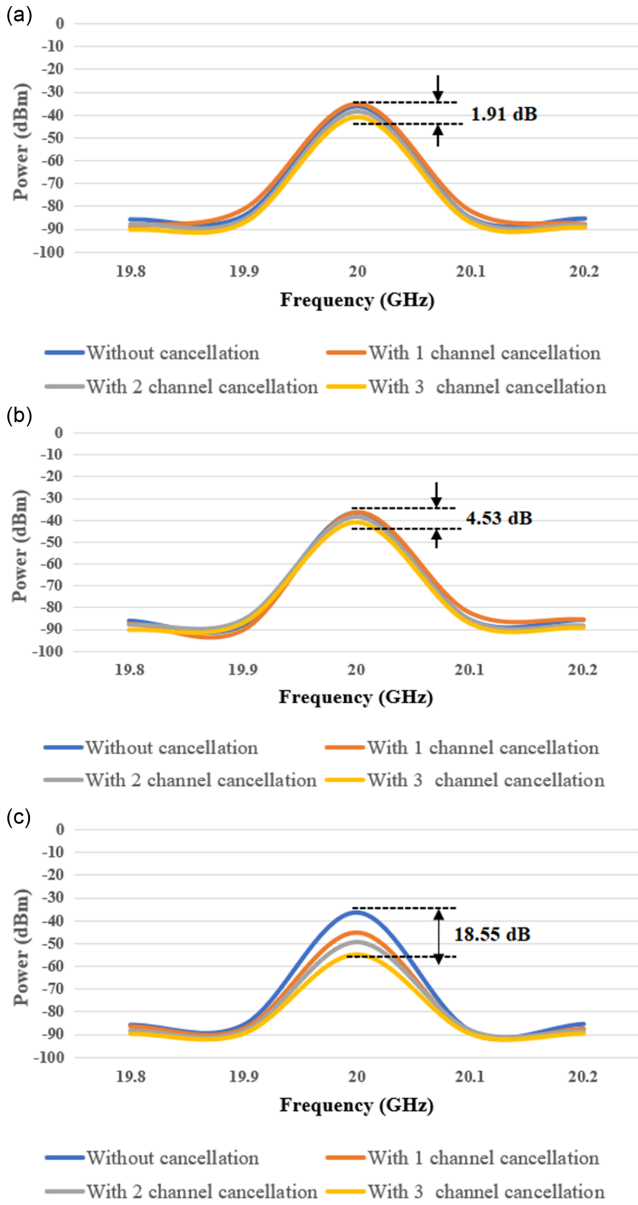


Figure 8

Electrical spectra obtained of different iterations of wideband multipath self-interference cancellation at carrier frequency of 20 GHz and bandwidth of 500 MHz, under (a) 1 cancellation channel, (b) 2 cancellation channels, and (c) 3 cancellation channels

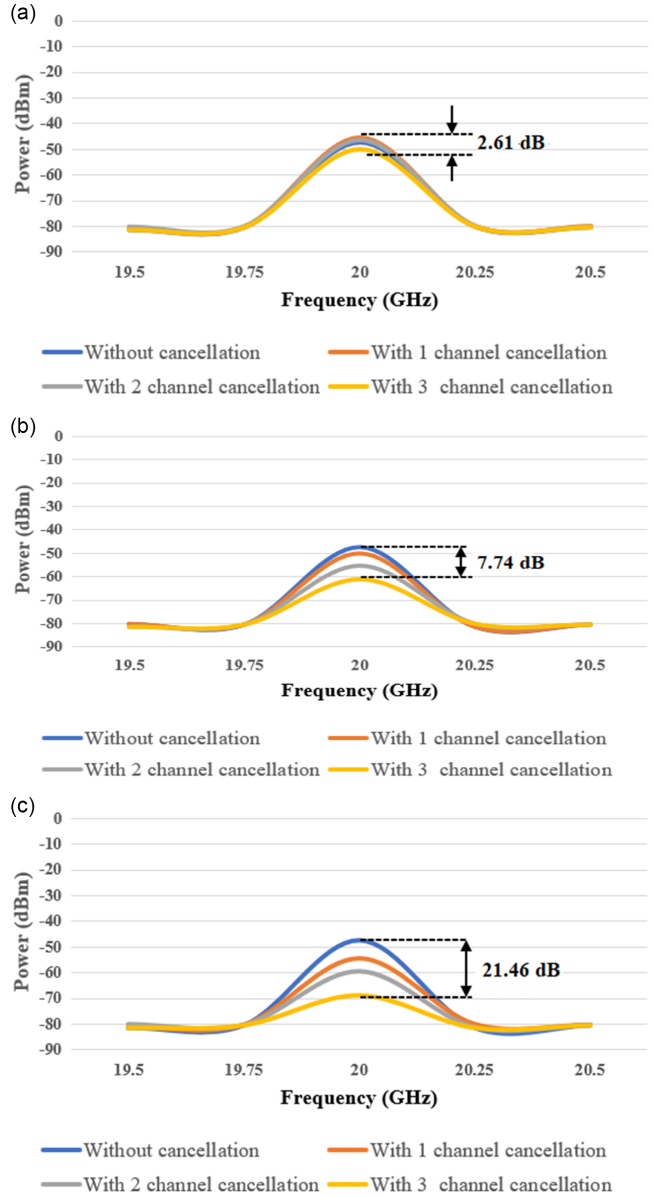


Table 1

Comparison of MSI cancellation depth obtained for signal with center frequency 20 GHz and different bandwidths vs different number of cancellation channels

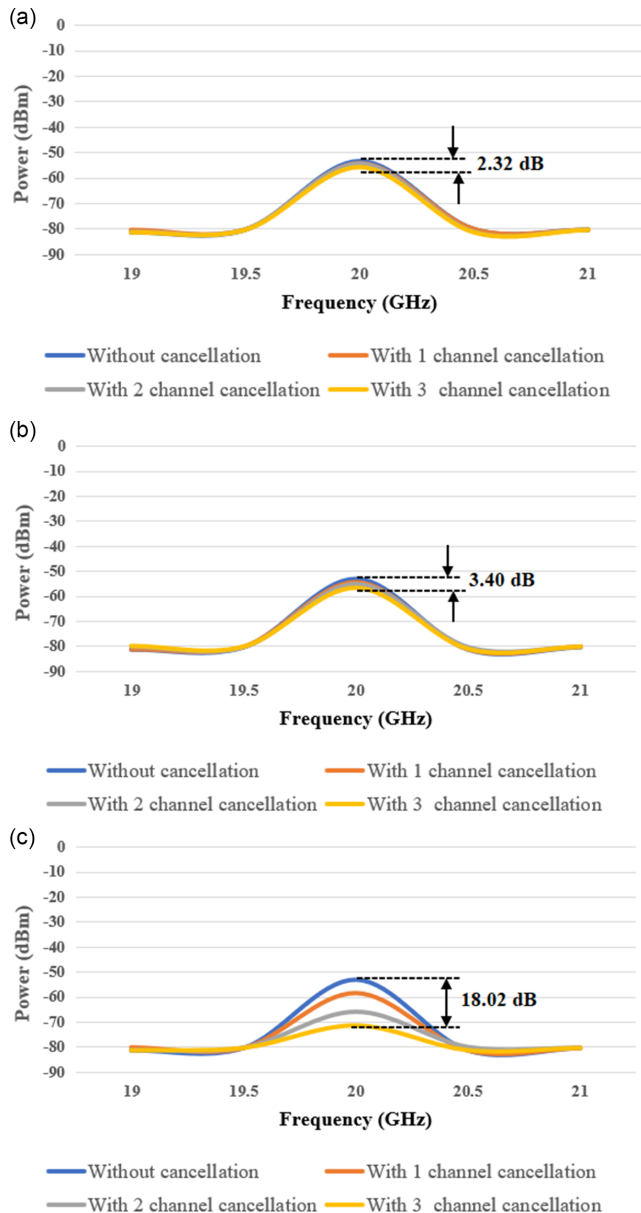
Bandwidth	No. of channel = 1	No. of channel = 2	No. of channel = 3
100 MHz	2.02 dB	6.04 dB	32.92 dB
200 MHz	1.91 dB	4.53 dB	18.58 dB
500 MHz	32.94 dB	18.58 dB	21.46 dB
1 GHz	2.32 dB	5.58 dB	18.02 dB

MSI cancellation performance. The time delay accuracy of OVDL, attenuation accuracy of OVA, phase matching of signals, and power control are acknowledged as important determining factors of wideband MSI cancellation. As the number of cancellation channels in OTMDL increases, sufficient cancellation of wideband MSI signals due to the Rayleigh fading channel is achieved. Proper tuning of OVDL and OVA is also a necessary condition for achieving better cancellation depths.

The Doppler shift can significantly influence the efficacy of SIC techniques. The sensitivity of the canceller to variations in Doppler frequency can diminish the performance of analog SIC, resulting in a

Figure 9

Electrical spectra obtained of different iterations of wideband multipath self-interference cancellation at carrier frequency of 20 GHz and bandwidth of 1 GHz, under (a) 1 cancellation channel, (b) 2 cancellation channels, and (c) 3 cancellation channels



reduction in rate gain. Despite being considered negligible in traditional communication systems, the Doppler shift can adversely affect SIC, potentially compromising its capability and diminishing overall system performance.

This paper evaluates the performance of a proposed photonic architecture of MSI cancellation technique for IBFD RoF communication. The system's performance is evaluated for single-tone RF signals and wideband signals with various bandwidths. The cancellation depth is calculated for various cancellation channels of the proposed OTMDL module, with results showing that the maximum cancellation depth of 30.63 dB is obtained when 3 cancellation channels are used. For a single-tone signal at 20 GHz, a 47.94 dB cancellation depth is obtained for 3 channel

cancellation. For wideband signals, the best cancellation depths are 32.94, 18.55, 21.46, and 18.02 dB for signals at 20 GHz with bandwidths of 100 MHz, 200 MHz, 500 MHz, and 1 GHz, respectively. The effectiveness of MSI cancellation can be improved by fine-tuning the optical components in OTMDL to effectively couple LR signals and digitally generated MSI signals. The proposed technology improves spectrum utilization, doubles data rates, and enhances overall performance, making it a key technology for next-generation wireless, radar, and sensor communication.

## 5. Conclusion

This paper proposes a photonics-assisted MSI cancellation technique for the IBFD RoF communication system under the Rayleigh fading channel. The system's performance is evaluated for single-tone RF signals and wideband signals with various bandwidths. The cancellation depth is calculated for various cancellation channels of the proposed OTMDL module, with results showing that the maximum cancellation depth of 30.63 dB is obtained when 3 cancellation channels are used. For a single-tone signal at 20 GHz, a 47.94 dB cancellation depth is obtained for 3 channel cancellation. For wideband signals, the best cancellation depths are 32.94, 18.55, 21.46, and 18.02 dB for signals at 20 GHz with bandwidths of 100 MHz, 200 MHz, 500 MHz, and 1 GHz, respectively. The performance of the proposed technology is constrained by the accuracy of the designed OTMDL module, the nonlinear interaction of electronic devices used, and phase noise introduced in the optical system. However, the effectiveness of MSI cancellation can be improved by fine-tuning the optical components in OTMDL to effectively couple LR signals and digitally generated MSI signals. The proposed photonic architecture of MSI cancellation technique for IBFD RoF communication is a key technology for next-generation wireless, radar, and sensor communication that improves spectrum utilization, doubles data rates, and enhances overall performance.

## Ethical Statement

This study does not contain any studies with human or animal subjects performed by any of the authors.

## Conflicts of Interest

The authors declare that they have no conflicts of interest to this work.

## Data Availability Statement

Data available on request from the corresponding author upon reasonable request.

## References

- [1] Chen, Y., Ding, C., Jia, Y., & Liu, Y. (2022). Antenna/propagation domain self-interference cancellation (SIC) for in-band full-duplex wireless communication systems. *Sensors*, 22(5), 1699. <https://doi.org/10.3390/s22051699>
- [2] Ahmed, M. A., Tsimenidis, C. C., & Al Rawi, A. F. (2016). Performance analysis of full-duplex-MRC-MIMO with self-interference cancellation using null-space-projection. *IEEE Transactions on Signal Processing*, 64(12), 3093–3105. <https://doi.org/10.1109/TSP.2016.2540611>

- [3] Kang, Y. Y., Kwak, B. J., & Cho, J. H. (2014). An optimal full-duplex AF relay for joint analog and digital domain self-interference cancellation. *IEEE Transactions on Communications*, 62(8), 2758–2772. <https://doi.org/10.1109/TCOMM.2014.2342230>
- [4] Khaledian, S., Farzami, F., Smida, B., & Erricolo, D. (2018). Inherent self-interference cancellation for in-band full-duplex single-antenna systems. *IEEE Transactions on Microwave Theory and Techniques*, 66(6), 2842–2850. <https://doi.org/10.1109/TMTT.2018.2818124>
- [5] Venkatakrishnan, S. B., Alwan, E. A., & Volakis, J. L. (2018). Wideband RF self-interference cancellation circuit for phased array simultaneous transmit and receive systems. *IEEE Access*, 6, 3425–3432. <https://doi.org/10.1109/ACCESS.2017.2788179>
- [6] Xu, W., Liang, L., Zhang, H., Jin, S., Li, J. C., & Lei, M. (2012). Performance enhanced transmission in device-to-device communications: Beamforming or interference cancellation? In *IEEE Global Communications Conference*, 4296–4301. <https://doi.org/10.1109/GLOCOM.2012.6503793>
- [7] Zhou, Q., Feng, H., Scott, G., & Fok, M. P. (2014). Wideband co-site interference cancellation based on hybrid electrical and optical techniques. *Optics Letters*, 39(22), 6537–6540. <https://doi.org/10.1364/OL.39.006537>
- [8] van den Broek, D. J., Klumperink, E. A., & Nauta, B. (2015). An in-band full-duplex radio receiver with a passive vector modulator downmixer for self-interference cancellation. *IEEE Journal of Solid-State Circuits*, 50(12), 3003–3014. <https://doi.org/10.1109/JSSC.2015.2482495>
- [9] Kargaran, E., Tijani, S., Pini, G., Manstretta, D., & Castello, R. (2017). Low power wideband receiver with RF self-interference cancellation for full-duplex and FDD wireless diversity. In *IEEE Radio Frequency Integrated Circuits Symposium*, 348–351. <https://doi.org/10.1109/RFIC.2017.7969089>
- [10] Korpi, D., Venkatasubramanian, S., Riihonen, T., Anttila, L., Otewa, S., Icheln, C., . . . , & Wichman, R. (2013). Advanced self-interference cancellation and multi-antenna techniques for full-duplex radios. In *Asilomar Conference on Signals, Systems and Computers*, 3–8. <https://doi.org/10.1109/ACSSC.2013.6810217>
- [11] Urlick, V. J., Godinez, M. E., & Mikeska, D. C. (2020). Photonic assisted radio-frequency interference mitigation. *Journal of Lightwave Technology*, 38(6), 1268–1274. <https://doi.org/10.1109/JLT.2019.2955921>
- [12] Han, X., Su, X., Fu, S., Gu, Y., Wu, Z., Li, X., & Zhao, M. (2021). RF self-interference cancellation by using photonic technology. *Chinese Optics Letters*, 19(7), 073901. <https://doi.org/10.3788/COL202119.073901>
- [13] Du, Y., Yang, K., Li, G. F., Chen, N., & Liu, S. (2023). Single antenna and no circulator full-duplex with 52 dB wideband self-interference suppression. *IEEE Transactions on Circuits and Systems I: Regular Papers*, 70(9), 3451–3460. <https://doi.org/10.1109/TCSI.2023.3247744>
- [14] Gao, C., Zhu, Z., Li, H., Wang, G., Zhou, T., Li, X., . . . , & Zhao, S. (2023). A fiber-transmission-assisted fast digital self-interference cancellation for overcoming multipath effect and nonlinear distortion. *Journal of Lightwave Technology*, 41(22), 6898–6907. <https://doi.org/10.1109/JLT.2023.3304588>
- [15] Hong, Z. H., Zhang, L., Wu, Y., Li, W., Park, S. I., Ahn, S., . . . , & Angueira, P. (2024). Iterative successive nonlinear self-interference cancellation for in-band full-duplex communications. *IEEE Transactions on Broadcasting*, 70(1), 2–13. <https://doi.org/10.1109/TBC.2023.3291136>
- [16] Yu, X., Ye, J., Yan, L., Zhou, T., Zhu, Y., Li, P., . . . , & Pan, W. (2023). Photonic-assisted adaptive multipath self-interference cancellation using deep reinforcement learning. *Journal of Lightwave Technology*, 41(23), 7183–7191. <https://doi.org/10.1109/JLT.2023.3307810>
- [17] Chen, S., Qi, H., Ye, L., Meng, W., & Li, C. (2023). Performance analysis and optimization of zero-setting OFDM in full-duplex relay system. In *IEEE International Conference on Communications*, 216–221. <https://doi.org/10.1109/ICC45041.2023.10279705>
- [18] Kim, D., Lee, H., & Hong, D. (2015). A survey of in-band full-duplex transmission: From the perspective of PHY and MAC layers. *IEEE Communications Surveys & Tutorials*, 17(4), 2017–2046. <https://doi.org/10.1109/COMST.2015.2403614>
- [19] Zhang, Y., Xiao, S., Feng, H., Zhang, L., Zhou, Z., & Hu, W. (2015). Self-interference cancellation using dual-drive Mach-Zehnder modulator for in-band full-duplex radio-over-fiber system. *Optics Express*, 23(26), 33205–33213. <https://doi.org/10.1364/OE.23.033205>
- [20] Gong, C., & Xu, Z. (2015). Channel estimation and signal detection for optical wireless scattering communication with inter-symbol interference. *IEEE Transactions on Wireless Communications*, 14(10), 5326–5337. <https://doi.org/10.1109/TWC.2015.2436398>
- [21] Bashir, M. S., & Alouini, M. S. (2021). Optimal power allocation between beam tracking and symbol detection channels in a free-space optical communications receiver. *IEEE Transactions on Communications*, 69(11), 7631–7646. <https://doi.org/10.1109/TCOMM.2021.3099838>
- [22] Yuan, J., Sang, X., Yu, C., Han, Y., Zhou, G., Li, S., & Hou, L. (2011). Highly efficient and broadband Cherenkov radiation at the visible wavelength in the fundamental mode of photonic crystal fiber. *IEEE Photonics Technology Letters*, 23(12), 786–788. <https://doi.org/10.1109/LPT.2011.2136431>
- [23] Delmade, A., Browning, C., Farhang, A., Koilpillai, R. D., Venkitesh, D., & Barry, L. P. (2019). OFDM baud rate limitations in an optical heterodyne analog fronthaul link using unlocked fibre lasers. In *International Topical Meeting on Microwave Photonics*, 1–4. <https://doi.org/10.1109/MWP.2019.8892190>

**How to Cite:** Chandrasenan, A., & Zacharias, J. (2024). A Multipath Approach to Self-Interference Cancellation in MIMO Rayleigh Fading Channels. *Journal of Optics and Photonics Research*, 1(2), 82–90. <https://doi.org/10.47852/bonview/JOPR32021772>